Articles

Red Fox Ancestry and Connectivity Assessments Reveal Minimal Fur Farm Introgression in Greater Yellowstone Ecosystem

Patrick R. Cross,* Benjamin N. Sacks, Gordon Luikart, Michael K. Schwartz, Keith W. Van Etten, Robert L. Crabtree

P.R. Cross, K.W. Van Etten, R.L. Crabtree

Yellowstone Ecological Research Center, 2048 Analysis Drive Suite B, Bozeman, Montana 59718

P.R. Cross, R.L. Crabtree

Systems Ecology Program, College of Forestry and Conservation, University of Montana, 32 Campus Drive, Missoula, Montana 59812

B.N. Sacks

Mammalian Ecology and Conservation Unit, Veterinary Genetics Laboratory, School of Veterinary Medicine, University of California Davis, 1 Shields Avenue, Davis, California 95616

G. Luikart

Flathead Lake Biological Station, Montana Conservation Genomic Laboratory, Division of Biological Sciences, University of Montana, 32125 Bio Station Lane, Polson, Montana 59860

M.K. Schwartz

National Genomics Center for Wildlife and Fish Conservation, U.S. Department of Agriculture, Forest Service, 32 Campus Drive, Missoula, Montana 59812

Abstract

Rocky Mountain red foxes *Vulpes vulpes macroura* potentially encounter other red fox *Vulpes vulpes* lineages at lower elevations, which may include nonindigenous red foxes derived from fur farms. Introgression from nonindigenous red foxes could have negative evolutionary consequences for the rare Rocky Mountain red fox subspecies. Red foxes at high elevations in the Greater Yellowstone Ecosystem exhibit lighter coat colors than those at lower elevations, potentially indicating that they represent the indigenous subspecies and that gene flow across the elevational gradient is restricted. We collected tissue samples across a 1,750-m elevation range and examined mitochondrial DNA sequences and nuclear DNA microsatellite genotypes to assess the ancestry and genetic population structure of red foxes in the northern Greater Yellowstone Ecosystem. We also used reference samples from fur farm red foxes and indigenous red foxes of the western United States to assess the extent of nonindigenous introgression across the ecosystem. We found little overlap in the elevational distribution of maternally inherited mitochondrial DNA haplotypes: above 1,600 m, we only found indigenous Rocky Mountain haplotypes ($n = 4$), whereas below 1,600 m, we found haplotypes not indigenous to the Rocky Mountains ($n = 5$) that were associated with fur farms or indigenous to the Great Plains. In contrast, biparentally inherited microsatellite variation showed little population structure across the elevational gradient. Despite this evidence of nuclear gene flow across the elevational gradient, we found little fur farm introgression in the microsatellite genotypes. It is possible that long-standing nuclear (but apparently not mitochondrial) gene flow between Rocky Mountain red foxes and indigenous red foxes on the Great Plains explained the low nuclear differentiation of these populations. Importantly, our results suggested that high elevations of the northern Greater Yellowstone Ecosystem remained free of significant fur farm introgression. Mitonuclear discordance could reflect sex-biased dispersal, which we hypothesize could be the effect of elevational differences in reproductive phenology.

The findings and conclusions in this article are those of the author(s) and do not necessarily represent the views of the U.S. Fish and Wildlife Service.

* Corresponding author: cross@yellowstoneresearch.org

Introduction

Major mountain ranges in the western United States harbor endemic red fox *Vulpes vulpes* subspecies collectively known as montane red foxes: Sierra Nevada red fox *Vulpes vulpes necator* in the Sierra Nevada and Oregon Cascades, Cascade red fox *Vulpes vulpes cascadensis* in the Washington Cascades, and Rocky Mountain red fox *Vulpes vulpes macroura* in the Rocky Mountains (Hall and Kelson 1959; Kamler and Ballard 2002; Aubry et al. 2009; Sacks et al. 2010). Montane red foxes share a common ancestor that colonized North America via Beringia before the Illinoian Glaciation (~191–130 kya) up to 500 kya, but these red foxes became reproductively isolated in their respective subalpine habitat islands after the end of the Pleistocene (Aubry et al. 2009; Statham et al. 2014). Red foxes at lower elevations in the western United States, in contrast, may comprise a mixture of expanding montane red foxes, other indigenous red foxes that derive from either the pre-Illinoian Glaciation colonization or from a later colonization event during the Wisconsin Glaciation (100–10 kya), or nonindigenous red foxes associated with fur farms (Kamler and Ballard 2002; Aubry et al. 2009; Sacks et al. 2010, 2016; Statham et al. 2012; Volkmann et al. 2015). In the early 19th century, explorers Meriwether Lewis and Prince Maximilian von Weid observed red foxes along the Missouri River at elevations below 750 m (Moulton 2005; Witte and Gallagher 2012); but today, most low-elevation red foxes probably derive at least partly from fur farm red foxes (Volkmann et al. 2015; Merson et al. 2017). Fur farm red foxes, which were subject to captive breeding for many generations, derive primarily from eastern North American red foxes (which also originated before the Illinoian Glaciation) and Alaskan red foxes (which originated during the Wisconsin Glaciation), and they were augmented with breeding stock from the Washington Cascades (Sacks et al. 2016; Lounsberry et al. 2016; Merson et al. 2017).

Introgression from low-elevation red foxes could therefore have negative effects on indigenous montane red foxes including the loss of locally adaptive traits, outbreeding depression, and, in the case of extreme genetic swamping, the alteration of functional ecological roles (Allendorf et al. 2001; Carbyn and Watson 2001; Sacks et al. 2011; Champagnon et al. 2012). The risk of these threats may be increasing given that most of the studied montane red foxes appear to be declining as nonindigenous and admixed red foxes expand (Perrine et al. 2007, 2010; Sacks et al. 2010; Statham et al. 2012; Volkmann et al. 2015; Sacks et al. 2016). For example, the U.S. Fish and Wildlife Service (USFWS) recently determined that a Sierra Nevada red fox population in California was a candidate for endangered or threatened species protection under the U.S. Endangered Species Act (ESA 1973, as amended), citing "threats from hybridization with nonnative red fox" (USFWS 2015). Over the time that this indigenous population declined in both range and size, nonindigenous red foxes in California expanded to cover a nearly continuous distribution at lower elevations (USFWS 2015; Sacks et al. 2016). Understanding the distributions of and interactions between indigenous and nonindigenous red foxes is therefore important for the conservation of North America's indigenous montane red foxes.

Wide phenotypic variation among individual red foxes can make it difficult to visually distinguish indigenous, nonindigenous, and admixed individuals (Volkmann et al. 2015). In 1881, before the proliferation of fur farms in the western United States, Yellowstone National Park superintendent P.W. Norris described its indigenous red foxes as "numerous and of various colors, the red, grey, black, and the cross varieties (most valuable of all) predominating in the order named" (Fuhrmann 1998). Yet above 2,300 m in the Greater Yellowstone Ecosystem (GYE), red foxes exhibit a significant frequency of blonde and gray pelages (Figure 1) that are lighter than the common red pelage more frequent at lower elevations (Crabtree 1998; Fuhrmann 1998; Swanson et al. 2005). These high-elevation red foxes possess other traits that are beneficial in a montane environment, such as large, fur-covered feet that Fuhrmann (1998) calculated to have over-snow weight loading capabilities comparable to those of Canada lynx *Lynx canadensis*. Swanson et al. (2005) also detected significant genetic differentiation between red foxes from three elevation groups in the GYE: above 2,300 m where lighter coat colors are frequent; between 2,300 m and 1,600 m where montane habitats transition into nonmontane habitats; and below 1,600 m where nonmontane habitats including agricultural and urban development dominate the landscape. These findings suggest that high-elevation red foxes in the GYE are a

Figure 1. A Rocky Mountain red fox *Vulpes vulpes macroura* carrying 11 northern pocket gophers *Thomomys talpoides* along the Beartooth Highway near Top of the World, Wyoming, on May 24, 2012 (photo, P.R. Cross). This Rocky Mountain red fox, photographed at 2,912-m elevation, displays a blonde and gray coat color that, above 2,300 m in the Greater Yellowstone Ecosystem, occurs at a significantly greater frequency than the red coat color common at lower elevations (Swanson et al. 2005). He was retrieving prey caught in roadside meadows and cached in the snow bank along the recently plowed highway, to provision a den at 2,875 m.

remnant population of the Rocky Mountain subspecies and that gene flow between these elevational groups is restricted despite the continuous distribution of red foxes across the ecosystem and the absence of geographic barriers between elevation groups (Fuhrmann 1998; Swanson et al. 2005).

Our primary objective was to test the hypotheses of Fuhrmann (1998) and Swanson et al. (2005) that the GYE's high-elevation red foxes are indigenous and genetically isolated by assessing the ancestry and the genetic diversity and population structure of red foxes across a 1,750-m elevational gradient in the northern GYE. To determine whether any elevational gene flow was natural or anthropogenic, we also assessed the extent of fur farm red fox introgression across the ecosystem. For matrilineal ancestry, we compared mitochondrial DNA (mtDNA) sequences from samples collected across three elevation groups in the GYE to haplotypes cataloged in a previous phylogeographic study (Aubry et al. 2009). For genetic diversity and population structure, we used nuclear DNA (nuDNA) microsatellite genotypes from our GYE samples to estimate diversity metrics and conduct assignment tests. We also investigated sex-biased gene flow by using population differentiation estimates (F_{ST}) from both maternally inherited mtDNA and biparentally inherited nuDNA, as that could help explain differences between results based on mtDNA sequences or microsatellite genotypes. And to assess fur farm introgression and paternal ancestry in the GYE, we performed an additional assignment test after adding genotypes from reference samples of known origin from fur farm red foxes and indigenous red foxes from other Rocky Mountain populations (Sacks et al. 2010, 2016). These reference

samples provided a broader phylogenetic context than was available for the previous GYE studies.

Methods

Samples

We collected tissue samples from red foxes in the northern GYE (Figure 2) across the three elevation groups defined by Swanson et al. (2005): high (>2,300 m; $n = 10$), middle (1,600–2,300 m; $n = 11$), and low (<1,600 m; $n = 7$). Our high-elevation area was centered on Beartooth Lake (44.945°N, 109.589°W) in the Shoshone National Forest, Wyoming. The middle-elevation area was centered on the Lamar Valley (44.898°N, 110.256°W) in Yellowstone National Park, Wyoming, approximately 55 km west of Beartooth Lake. The low-elevation area surrounded the high- and middle-elevation areas within a 150-km radius of the high-elevation area. Land cover ranged from alpine tundra and subalpine forests and parklands at high elevations to montane forests and sagebrush steppe at middle elevations to xeric plains, riparian corridors, and developed lands at low elevations.

For the high-elevation group, we obtained tissue samples primarily through live trapping. We used number 1.5 soft catch, center swivel, padded steel leghold traps (Woodstream Corp., Lititz, PA) and plywood box traps measuring 0.46 m wide, 0.6 m high, and 1.22 m long (Keith Van Etten, Cooke City, MT) for 1 mo in spring 2012 (308 trap nights; one capture); log cabin traps (Figure 3; Copeland et al. 1995) built on site measuring 1 m wide, 1 m high, and 1.75 m long for 3 mo in winter 2013 (115 trap nights; eight captures including four recaptures); and log cabin traps for 3 mo in winter 2014 (173 trap nights; four captures including one recapture). By spacing traps about 2 km apart along a 12-km trapline, we expected to target up to 25 individual red foxes, assuming a continuous distribution of 4-km² territories each with a resident breeding pair and one "helper" yearling female (Hersteinsson and Macdonald 1982; Fuhrmann 1998; Crabtree and Sheldon 1999). We restrained captured red foxes without chemical immobilization by using an animal control pole (Ketch-All, San Luis Obispo, CA); wood chomp bit; and electrical tape securing the jaws, a blindfold, electrical tape securing the feet, and a heavy blanket. We then collected a tissue sample with an ear punch, applied a topical antiseptic (Dr. Naylor, Morris, NY) to the collection site, and preserved the sample in ethanol or silica desiccant. For the middle-elevation group, we used samples that were collected between 2003 and 2005 for a previous study (Van Etten et al. 2007) by using leghold and box traps and with the handling methods described above. These trapping and handling methods, which avoid the physiological side effects of chemical immobilization, followed American Society of Mammalogists guidelines and were previously approved by the Colorado State University Animal Care and Use Committee (Van Etten et al. 2007; Sikes et al. 2011). For the entire low-elevation
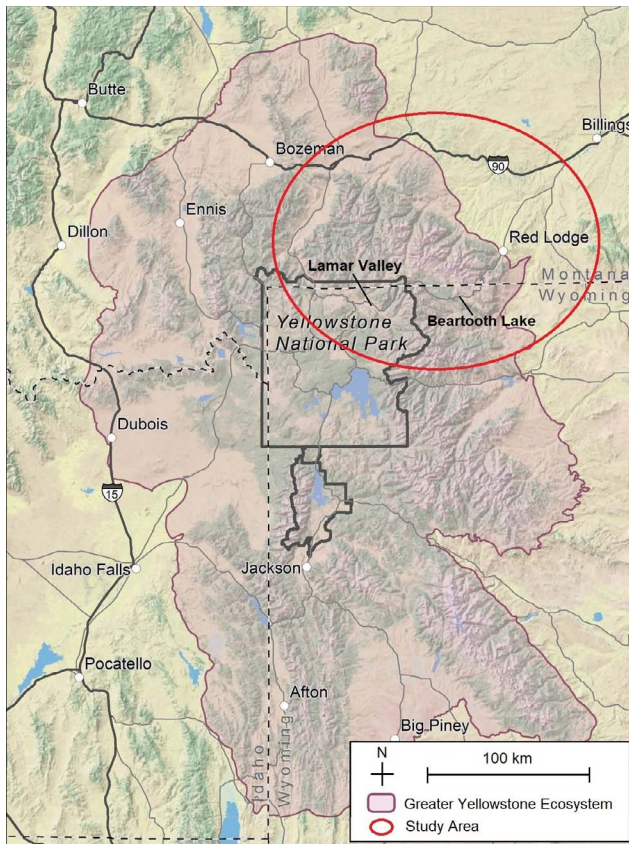
Figure 2. Map of the Greater Yellowstone Ecosystem in Montana, Wyoming, and Idaho, with the study area where we collected red fox *Vulpes vulpes* tissue samples between 2003 and 2016 circled in red. Background image courtesy of the U.S. Geological Survey–Interagency Grizzly Bear Study Team.

Figure 3. Camera trap image of a log cabin trap on the Beartooth Plateau in northwestern Wyoming, with a Rocky Mountain red fox *Vulpes vulpes macroura* about to enter it on March 16, 2013 (photo, P.R. Cross). We predominantly used this type of trap in our sample collection.

group, as well as to supplement the high- and middle-elevation groups, we collected tissue samples opportunistically between 2012 and 2016 from fur trappers ($n = 2$) and roadkill ($n = 6$): snow plow drivers, local law enforcement, and area newspaper readers assisted in this effort.

The fur farm reference samples were collected in California ($n = 24$) for a previous study (Sacks et al. 2016). Even though we did not have samples from local fur farms, these California samples nevertheless provided a valid nonindigenous fur farm reference due to the shared ancestry of fur farm red foxes across North America (Sacks et al. 2016; Merson et al. 2017). The indigenous reference samples were collected in Idaho ($n = 16$) and Nevada ($n = 5$), also for a previous study (Sacks et al. 2010). Our GYE samples and these reference samples were all processed under the same procedures by the Mammalian Ecology and Conservation Unit at the University of California–Davis Veterinary Genetics Laboratory.

Laboratory procedures

We extracted DNA using the DNeasy tissue kit (Qiagen, Hilden, Germany) following the manufacturer's protocol. All but one sample from the middle-elevation group

yielded usable DNA. We sequenced a portion of the mtDNA cytochrome *b* gene by using primers RF14724 (5′-CAACTATAAGAACATTAATGACC-3′) and RF15149 (5′-CTCAGAATGATATTTGTCCTC-3′) to amplify via polymerase chain reaction (PCR) a 441-bp fragment, producing a 354-bp product after sequencing from RF14724 and trimming (Perrine et al. 2007). We also amplified and sequenced a portion of the D-loop to produce an ~400-bp product (depending on indels) by using primers VVDL1 (5′-TCCCCAAGACTCAAGGAAGA-3′) and VVDL6 (5′-CAGAATGGCCCTGAGGTAAG-3′), producing a 342-bp product after sequencing from the VVDL1 primer and trimming (Aubry et al. 2009). We sequenced fragments using BigDye Terminator v3.1 (Applied Biosystems, Foster City, CA) reagents and cycling conditions as described previously (Perrine et al. 2007; Aubry et al. 2009).

We genotyped samples at 28 nuDNA microsatellite loci (Table S1, *Supplemental Material*) in four multiplex reactions by using previously published primers (Ostrander et al. 1993, 1995; Holmes et al. 1998; Moore et al. 2010). We amplified markers via PCR of 1 μL of DNA (extract diluted 1:100 in sterile water), fluorescently labeled primers (6-FAM, VIC, NED, PET; Applied Biosystems), and Qiagen multiplex PCR kit reagents including "Q-solution," according to the manufacturer's protocol with annealing temperature set at 58°C. We electrophoresed PCR products along with an internal size standard, Genescan 500 LIZ (Applied Biosystems), on an ABI 3730 capillary sequencer (Applied Biosystems) and called alleles manually by using program Strand v.2.4.113 (Toonen and Hughes 2001). Our high-quality tissue samples yielded clearly defined genotypes, so we accepted initial genotype scores without double-scoring, while we manually scanned through allele calls to ensure

consistency between our GYE dataset and the reference dataset.

Relatedness

We first used microsatellite genotypes to identify closely related individuals within each elevation group by using ML-Relate (Kalinowski et al. 2006), given that their inclusion could lead to overestimates of population structure (Gariboldi et al. 2016; Oklander et al. 2017; but see Waples and Anderson 2017). After estimating the putative relationship (parent-offspring, full-sibling, half-sibling, or unrelated) between each pair of samples based on maximum likelihood, we conducted likelihood ratio tests against alternative hypotheses (e.g., full-sibling for any putative parent-offspring pair) in 200,000 simulations to assess whether the putative relationship fit the data better than the alternative relationship, disregarding any putative relationship with an insignificant ($P > 0.05$) difference. We then created a data subset that excluded one individual from each remaining pair of first-order relatives (the offspring in any parent-offspring pair, and a randomly selected sibling in any full-sibling pair) and tested it against the dataset with all samples to determine whether including first-order relatives would cause an overestimate of population structure. To do this, we used Genepop 4.3 (Rousset 2008) to compare pairwise F_{ST} for the three elevation groups within each respective dataset, expecting different F_{ST} estimates if the inclusion of first-order relatives affected population structure estimates. We then chose the dataset with the most conservative population structure estimates (i.e., lowest F_{ST} estimates) for subsequent analyses of genetic diversity and population structure.

Matrilineal ancestry and genetic diversity

We combined sequence data from the linked mtDNA cytochrome *b* gene and D-loop into a composite haplotype for each sample and compared these to previously published reference haplotypes using the same nomenclature: alphabetic or alphanumeric cytochrome *b* component, hyphen, numeric D-loop component (e.g., A-43 and A3-59; Sacks et al. 2010). These reference haplotypes were drawn from historical (pre-1940) specimens collected across the red fox's circumboreal range, and they phylogenetically fall into two distinct clades: (1) the Nearctic clade that originated in North America before the Illinoian Glaciation, further divided into the "mountain" and "eastern" subclades, and (2) the Holarctic clade that entered North America during the Wisconsin Glaciation (Aubry et al. 2009). These haplotypes have been used to identify red foxes of indigenous and nonindigenous (i.e., fur farm) ancestry in other studies across North America (reviewed by Merson et al. 2017). To visualize mtDNA structure in this sample, we constructed a median-joining network of observed haplotypes by using Network 5.0 (Fluxus Engineering, Clare, Suffolk, UK), weighting substitutions on the

cytochrome *b* component twice those on the faster mutating D-loop component (Bandelt et al. 1999; Sacks et al. 2010; Merson et al. 2017). We calculated haplotype diversity for each elevation group with Arlequin 3.5.2.2 (Excoffier et al. 2005) and mtDNA F_{ST} among elevation groups with Genepop 4.3.

Nuclear genetic diversity, population structure, and ancestry

Using microsatellite genotypes and Genepop 4.3, we calculated expected heterozygosity (*He*) and observed heterozygosity (*Ho*) and tested for deviations from Hardy–Weinberg proportion (HWP; assessed by using F_{IS} estimates relating the population's average deviation from HWP) and linkage disequilibrium (LD) among loci within each elevation group. Because our sample size was small, we had low power to detect deviations from HWP or to detect LD. Therefore, to be conservative (i.e., more likely to detect deviations when none actually existed), we did not correct for multiple tests. We assessed genetic diversity by comparing overall allelic richness and richness of private alleles for all elevation group pairs calculated using HP-Rare, a statistical technique that uses rarefaction to adjust for differences in sample size (Kalinowski 2005). We used Genepop 4.3 to estimate nuDNA F_{ST} among elevation groups. Together with mtDNA F_{ST} estimates, we used these nuDNA F_{ST} estimates to estimate the ratio of male-to-female migrants per generation between elevation groups to investigate sex-biased gene flow (Hedrick et al. 2013).

Next, we assessed genetic population structure. We first examined the effect of isolation by distance (IBD; Wright 1943) by using individual-based Mantel tests for correlation between genetic distance (the proportion of shared alleles [Bowcock et al. 1994] calculated with the "adegenet" R package) and both geographic and elevational distances, performed with the "ecodist" R package (Goslee and Urban 2007; Jombart 2008; R Core Team 2013). Then, we performed assignment tests with Structure 2.3.4 (Pritchard et al. 2000). To determine whether more than one discrete genetic cluster was present in our GYE dataset without imposing a priori elevation categories, we first performed a series of Structure runs with the number of clusters (*K*) ranging from one to six. We ran 10 iterations for every *K*-value, each with 100,000 repetitions following a 100,000 repetition burn-in period, by using the admixture model and correlated allele frequencies (Falush et al. 2003). We then used Structure Harvester to compute Δ*K*, a function of the standard deviation between iterations for each *K*-value and the rate of change in the natural log probability of the data [LnP(*K*)] between successive *K*-values (Evanno et al. 2005; Earl and vonHoldt 2012). After selecting the *K*-value with the greatest Δ*K* and mean LnP(*K*) to represent the most likely number of distinct clusters, we selected its iteration with the greatest LnP(*K*)

to estimate the proportion of ancestry (q) derived from a given cluster.

Finally, to assess nuclear ancestry and the effect of nonindigenous introgression, we performed an additional Structure analysis with $K = 2$ and the same parameters as mentioned above, but this time included the reference genotypes of known ancestry along with our GYE genotypes of unknown ancestry. We used the q-values from this Structure analysis to determine whether the GYE individuals were of indigenous red fox ancestry ($q > 0.85$ for the cluster corresponding with the indigenous reference samples), nonindigenous fur farm red fox ancestry ($q > 0.85$ for the cluster corresponding with the fur farm red fox reference samples), or admixed ancestry ($0.15 < q < 0.85$ for either cluster). These thresholds are based on the 90% confidence interval for correct assignment of the reference samples of known ancestry (Merson et al. 2017).

Results

Relatedness

We identified three parent-offspring pairs and one full-sibling pair in the high-elevation group. All of these putative relationships fit the microsatellite genotype data (Table S2, *Supplemental Material*) significantly better than did their alternative relationships. Therefore, we removed the offspring (one of which was represented twice with both its mother and its father) and one of the full siblings from the data subset excluding first-order relatives. We then found lower F_{ST} estimates ($\pm$SE) between the high-elevation group and the middle- and low-elevation groups, respectively, in the data subset excluding first-order relatives ($F_{ST} = 0.007 \pm 0.011$, $F_{ST} = 0.020 \pm 0.014$) than in the dataset including all samples ($F_{ST} = 0.017 \pm 0.012$, $F_{ST} = 0.036 \pm 0.014$), indicating greater (and possibly biased) population structure estimates in the more inclusive dataset. We therefore used the more conservative data subset that excluded first-order relatives for subsequent analyses of genetic diversity and population structure. In addition to these first-order relatives, we also identified three putative second-order relative pairs (e.g., half-sibling, grandparent–grandchild, uncle–nephew relationships) in the high-elevation group and four putative second-order relative pairs in the middle-elevation group. We did not identify any related individuals in the low-elevation group.

Matrilineal ancestry and genetic diversity

We observed nine haplotypes in the combined mtDNA sequence fragments (Table S3, *Supplemental Material*), defined by 1 to 18 substitutions among 26 variable nucleotides, with a mean of 9.72 substitutions (Table 1; Figure 4). The average haplotype diversity estimates were 0.56 ($\pm$0.07) in the high-elevation group, 0.64 ($\pm$0.15) in the middle-elevation group, and 0.95 ($\pm$0.10) in the low-elevation group. The high- and middle-

elevation groups ($>$1,600 m) had exclusively indigenous Rocky Mountain haplotypes: A-19, A-43, A3-59, and A3-276, the last of which included a novel D-loop haplotype (i.e., 276; GenBank accession MF281057) that differed from the A3-59 haplotype by one substitution. The low-elevation group ($<$1,600 m) had the greatest haplotype diversity, including one indigenous Rocky Mountain haplotype (A-43), one montane haplotype historically from the Washington Cascades but associated with modern fur farms (O-24), three eastern haplotypes (F-9, F-12, F5-9), and one holarctic haplotype (N-277) with a novel D-loop haplotype (i.e., 277, GenBank accession MF281058) that differed from the fur farm haplotype N-7 by two substitutions. We did not detect any European haplotypes, nor have previous studies in the western United States (e.g., Statham et al. 2012; Volkmann et al. 2015; Merson et al. 2017), failing to support previous hypotheses (i.e., Kamler and Ballard 2002) that low-elevation red foxes in the western United States descended from European red foxes introduced along the U.S. East Coast in the 18th century.

Our F_{ST} estimates for mtDNA were correspondingly lower between high and middle elevations ($F_{ST} = 0.030$) than between high and low elevations ($F_{ST} = 0.170$) and middle and low elevations ($F_{ST} = 0.190$). Given the similarity between the high- and middle-elevation groups, we also estimated F_{ST} between the combined high- and middle-elevation groups and the low-elevation group ($F_{ST} = 0.197$). The SE calculations for these mtDNA F_{ST} estimates are not available because haplotypes represented single markers.

Nuclear genetic diversity, population structure, and ancestry

For microsatellite genotypes, He was similar among elevation groups, but Ho was higher in the middle-elevation group than in the other two groups, which had similar Ho to each other (Table 2). None of the elevation groups was significantly out of HWP ($F_{IS} = 0.081$; $P = 0.527$). Two individual loci were significantly out of HWP in the high-elevation group, and one was significantly out of HWP in the low-elevation group. Ten pairs of loci (2.64%) exhibited LD in the high-elevation group, eight pairs (2.12%) in the middle-elevation group, and two pairs (0.53%) in the low-elevation group. No individual loci were out of HWP in more than one group, nor did any pairs of loci exhibit LD in more than one group, suggesting deviations can be explained by substructure or by false positives due to not adjusting for multiple tests, rather than by null alleles or other locus-specific issues. After rarefaction, allelic richness was similar among elevation groups, although private allelic richness was greatest in the low-elevation group and least in the high-elevation group.

Relative to mtDNA, F_{ST} estimates for microsatellites were generally low, but as with mtDNA, the lowest F_{ST} estimate (which did not differ significantly from zero) was between the high- and middle-elevation groups (F_{ST}

Table 1. Mitochondrial DNA haplotypes detected among 27 red foxes *Vulpes vulpes* sampled across three elevation groups in the northern Greater Yellowstone Ecosystem in Montana and Wyoming between 2003 and 2016. Groups of haplotypes are identified as Rocky Mountain haplotypes associated with Rocky Mountain red foxes *Vulpes vulpes macroura* or non–Rocky Mountain haplotypes associated with other red foxes (Aubry et al. 2009).

Elevation (m)	Rocky Mountain haplotype				Non–Rocky Mountain haplotype				
	A-19	A-43	A3-59	A3-276	O-24	F-9	F-12	F5-9	N-277
High (>2,300)	—	5	5	—	—	—	—	—	—
Middle (1,600–2,300)	1	2	6	1	—	—	—	—	—
Low (<1,600)	—	1	—	—	1	1	1	1	2

$= 0.007 \pm 0.011$). The F_{ST} estimates were only slightly higher between the high- and low-elevation groups ($F_{ST} = 0.020 \pm 0.014$) and the middle- and low-elevation groups ($F_{ST} = 0.026 \pm 0.011$). However, because there was minimal differentiation between the high- and middle-elevation groups to begin with, we also estimated F_{ST} between the combined high- and middle-elevation groups and the low-elevation group ($F_{ST} = 0.022 \pm 0.009$) as we did with the mtDNA F_{ST} estimates. With these results and the methods described by Hedrick et al. (2013), we estimated a ratio of 4.4 male migrants per generation for every female migrant between the combined high- and middle-elevation groups and the low-elevation group, assuming similar effective population sizes between sexes and other assumptions described by Hedrick et al. (2013).

We detected significant IBD with both geographic distance (Mantel $r = -0.209$; $P = 0.019$) and elevational distance (Mantel $r = -0.166$; $P = 0.015$). However, these explanatory variables were themselves correlated (Mantel $r = 0.605$; $P = 0.001$). So, we also performed partial Mantel tests for each variable controlling for the opposite variable to attempt to determine which variable was most likely causative. But neither of these tests yielded significant results; therefore, we could not determine whether geographic distance alone, elevational distance alone, or both geographic and elevational distance together affected genetic distance in our sample.

Within our GYE dataset alone, we found the greatest ΔK and mean LnP(K) when $K = 2$, although $K = 1$ produced a nearly identical LnP(K) (Figure 5). Nevertheless, to specifically test whether individuals in the GYE formed two discrete genetic clusters corresponding to high and low elevations, we forced genotypes into two genetic clusters (i.e., conducted an analysis at $K = 2$) and visualized each individual's respective q-values as a pie chart plotted by sampling location on a digital elevation model (Figure 6). This analysis indicated predominantly high or low q-values, contrary to the expectation that most genotypes would have intermediate q-values had the dataset represented one panmictic population. One cluster only had high q-values (>0.85) among individuals in the high- and middle-elevation groups, whereas the other cluster had high q-values among individuals across all three elevation groups. Therefore, population structure did

not appear to correspond to elevational barriers to gene flow; instead, IBD may have been the primary driver of the population structure we observed.

After adding the reference samples of known ancestry (Table S2), our GYE samples of unknown ancestry predominantly clustered ($q > 0.85$) with the indigenous reference samples (Figure 7). This included all of the samples in the high-elevation group. One sample from the middle-elevation group with an A-43 mtDNA haplotype had some admixture with fur farm stock. Three low-elevation samples carrying the fur farm–associated O-24 haplotype and the novel N-277 haplotype, which is closely related to the fur farm–associated N-7 haplotype, had some admixture with fur farm stock (these samples were also the lowest and easternmost in the dataset). No GYE samples had "pure" fur farm ancestry.
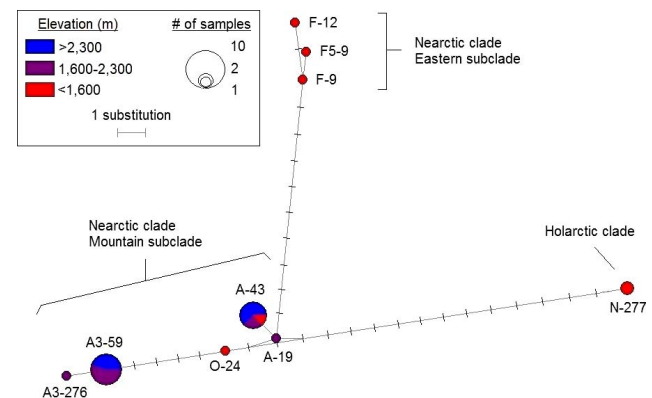

Figure 4. Network plot of cytochrome *b* and D-loop composite haplotypes detected among 27 red foxes *Vulpes vulpes* sampled in the northern Greater Yellowstone Ecosystem in Wyoming and Montana between 2003 and 2016. Haplotypes are individually labeled according to the nomenclature established in previous North American red fox studies (Sacks et al. 2010), whereas groups of haplotypes are labeled by previously identified clades (Aubry et al. 2009). These include the Nearctic clade that originated in North America before the Illinoian Glaciation (191–130 kya), which is geographically divided into Mountain and Eastern subclades, and the Holarctic clade that arrived in North America during the Wisconsin Glaciation (100–12 kya). Pie charts show the distribution of each haplotype among three elevational sampling groups: high ($n = 10$), middle ($n = 10$), and low ($n = 7$). We used these data to assess ancestry across the elevational gradient.

Table 2. Genetic diversity of 24 unrelated red foxes *Vulpes vulpes* sampled across three elevation groups in the northern Greater Yellowstone Ecosystem in Montana and Wyoming between 2003 and 2016, based on genotypes from 28 microsatellite loci. Data (with standard error [SE] estimates) include sample size (*n*), expected (*He*) and observed (*Ho*) heterozygosity, overall and private rarefied allelic richness (AR), and deviation from Hardy–Weinberg proportion test results (F_{IS}) and their *P*-values (significant when *P* < 0.05).

Elevation (m)	n	He ± SE	Ho ± SE	Overall AR ± SE	Private AR ± SE	F_{IS}	P
High (>2,300)	7[a]	0.70 ± 0.03	0.65 ± 0.04	4.30 ± 0.27	0.42 ± 0.10	0.05	0.53
Middle (1,600–2,300)	10	0.72 ± 0.03	0.74 ± 0.04	4.53 ± 0.30	0.64 ± 0.16	−0.01	0.63
Low (<1,600)	7	0.71 ± 0.03	0.67 ± 0.04	4.60 ± 0.36	0.87 ± 0.20	0.08	0.59

[a] We removed genotypes from three first-order relatives before analysis.

Discussion

Our findings supported the hypothesis that red foxes at high elevations in the GYE represented an indigenous population. We found little overlap in the distribution of mtDNA haplotypes, with exclusively indigenous Rocky Mountain red fox haplotypes above 1,600 m and a variety of nonmontane and nonindigenous haplotypes below 1,600 m. But low nuDNA F_{ST} estimates and evidence of weak population structure between high- and low-elevation populations indicated greater nuDNA gene flow across all elevations than previously reported (Swanson et al. 2005). Those results failed to support the hypothesis that the high-elevation red foxes were genetically isolated from those at lower elevations.

Of all the potential drivers of mitonuclear discordance such as we observed in our contrasting mtDNA and nuDNA results (reviewed in Toews and Brelsford 2012), male-biased dispersal across the elevation gradient seemed to be the most likely. Our finding of greater structuring in mtDNA compared to nuDNA and our estimate of male gene flow that was nearly 4.5 times greater than female gene flow, which was similar to previous estimates for red foxes (Sacks et al. 2016), support this conclusion. We hypothesize that synchrony between female reproductive physiology and local phenology prevents females entrained to low-elevation conditions from successfully recruiting kits at high elevations. Emergence from natal dens around the time of spring green-up (when weather conditions are mild and food availability is greatest) is likely adaptive, in which case deterministic reproductive events such as estrus and parturition should be timed accordingly. Spring green-up occurs later at higher elevations: 2014 Moderate Resolution Imaging Spectroradiometer (MODIS) phenology data and Snow Telemetry (SNOTEL) data showed spring conditions beginning roughly 2 mo later in our high-elevation area compared to our low-elevation area. In 2014, we also observed red fox kits at dens around 2,450 and 2,770 m that were less developed in June than kits observed a month earlier at 1,320 m, suggesting a corresponding difference in parturition time (P.R. Cross, unpublished data). This hypothesis could potentially be tested noninvasively by sampling urine across an elevation gradient to quantify reproductive hormones.

Despite the presence of nonmontane mtDNA haplotypes in the low-elevation area and the evidence of nuDNA gene flow across all elevations, our admixture
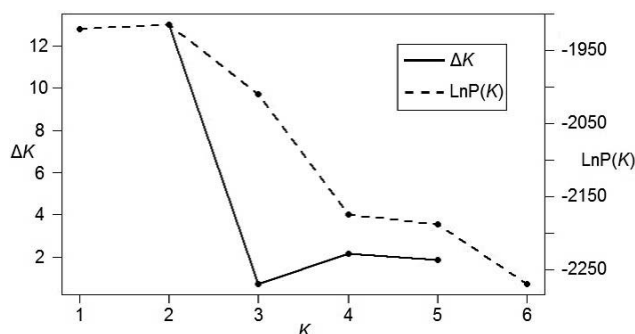

Figure 5. Assessments of the probability of the number of distinct clusters (*K*) among the genotypes of 24 unrelated red foxes *Vulpes vulpes* sampled in the northern Greater Yellowstone Ecosystem in Montana and Wyoming between 2003 and 2016, calculated with Structure Harvester (Earl and VonHoldt 2012) based on Structure (Pritchard et al. 2000) assignment test results.
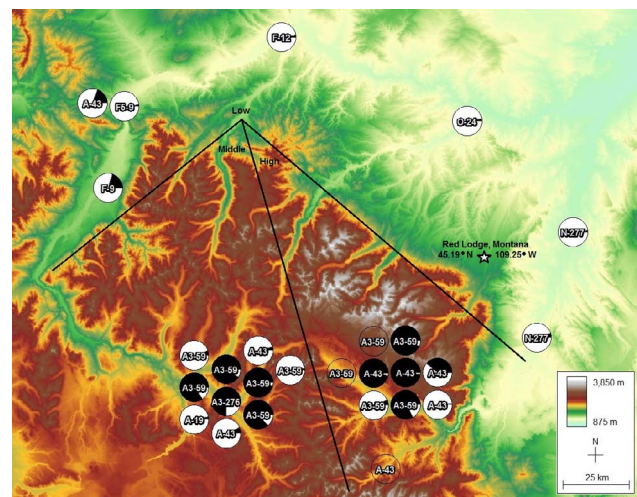

Figure 6. Geographic distribution of 27 red fox *Vulpes vulpes* tissue samples collected in the northern Greater Yellowstone Ecosystem in Montana and Wyoming between 2003 and 2016. Plotted on a 30-m digital elevation model, samples are labeled by mitochondrial DNA haplotype (Sacks et al. 2010) and divided by elevation group (high: >2,300 m; middle: 1,600–2,300 m; low: <1,600 m). Pie charts show proportion of assignment to each of *K* = 2 clusters determined from a Structure (Pritchard et al. 2000) assignment test of unrelated samples (*n* = 24). Unassigned (clear) samples are from first-order relatives (*n* = 3) whose genotypes we excluded from the assignment test.
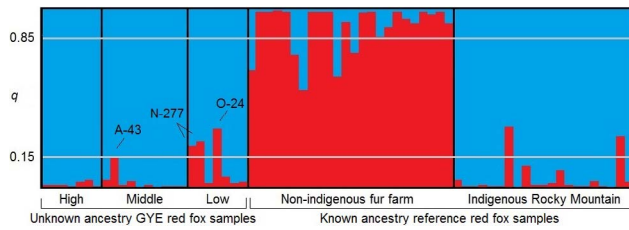
Figure 7. Structure (Pritchard et al. 2000) assignment test ($K = 2$) of 24 red fox *Vulpes vulpes* samples of unknown ancestry collected in the northern Greater Yellowstone Ecosystem (GYE) in Montana and Wyoming between 2003 and 2016, which are subdivided by elevation (high: >2,300 m; middle: 1,600–2,300 m; low: <1,600 m), along with 24 nonindigenous fur farm red fox reference samples collected in California between 1996 and 2010 (Sacks et al. 2016) and 21 indigenous red fox reference samples collected in the Rocky Mountains in Idaho ($n = 16$) and Nevada ($n = 5$) between 1880 and 2008 (Sacks et al. 2010). Cluster membership coefficient (q) thresholds for indigenous Rocky Mountain ancestry ($q < 0.15$), nonindigenous fur farm ancestry ($q > 0.85$), and admixed ancestry ($0.15 < q < 0.85$) are marked with gray lines. Mitochondrial DNA haplotype labels are included for admixed GYE samples.

analysis that included reference genotypes from fur farm red foxes found little evidence of fur farm introgression in the GYE as a whole, and none in the high-elevation group. All but one of the samples carrying indigenous Rocky Mountain red fox mtDNA haplotypes likewise had indigenous red fox nuDNA ancestry, whereas none of the samples, including those with mtDNA haplotypes associated with fur farms, had pure nonindigenous nuDNA ancestry. These results were similar to those of Merson et al. (2017) in Colorado in finding higher nuclear than mitochondrial gene flow across elevations. But they contrasted in that the gene flow from low-to-high elevations in Colorado reflected primarily fur farm introgression, whereas that in the present study appeared to be primarily indigenous Great Plains gene flow. Although it is possible that more sampling could detect individuals with greater fur farm introgression in the GYE, the minimal amount that we detected is notable especially considering the wide spatial distribution of the low-elevation group.

The three admixed individuals we sampled from the low-elevation group carried mtDNA haplotypes that were either associated with fur farms (i.e., O-24) or closely related to fur farm–associated haplotypes (i.e., N-277). In the early 20th century, there were fur farms with red foxes in Red Lodge, Montana (1,700 m), and Cody, Wyoming (1,520 m), close to where we found those three samples (Cole and Shackleford 1943; Clayton 2008). Red foxes that escaped or were released from these fur farms may have contributed to that introgression. Yet none of the foxes carrying eastern mtDNA haplotypes (F-9, F-12, F5-9) exhibited evidence of fur farm introgression. Although these haplotypes have been associated with fur farms (Merson et al. 2017), the western edge of their natural, historical distribution was unknown (Statham et al. 2012). Findings here suggest that they, and possibly the novel N-277 haplotype, may indeed derive from the

indigenous Great Plains lineages observed by Captain Lewis in 1805 and Prince Maximilian in 1834.

Therefore, our results support the persistence of indigenous red foxes at both high and low elevations in the GYE, and we suggest they reflect a natural coming-together of Rocky Mountain red foxes and indigenous red foxes of the Great Plains. Small amounts of fur farm admixture notwithstanding, the gene flow between these two prehistorically distinct indigenous populations presents a valuable study system for the evolutionary interplay between local adaptation and gene flow in the context of secondary contact. Future research could investigate the timescale of secondary contact between these two indigenous populations, whether it was during the Pleistocene or more recently, as well as genomic consequences of this secondary contact. Moreover, phylogeographic analyses of museum specimens and modern samples could help to clarify the present-day distribution of indigenous red foxes on the Great Plains as a whole. Compared to montane red foxes, those on the northern Great Plains have received little scientific attention. A better understanding of these low-elevation red foxes would benefit our knowledge of its contribution to population dynamics, locally adapted traits, and other distinguishing features of indigenous red foxes in the western United States. This is especially true in the GYE where red foxes indigenous to the Great Plains, along with Rocky Mountain red foxes, apparently remain an important part of a natural system.

Supplemental Material

Please note: The *Journal of Fish and Wildlife Management* is not responsible for the content or functionality of any supplemental material. Queries should be directed to the corresponding author for the article.

Table S1. Microsatellite loci used to assess relatedness, genetic diversity, genetic population structure, and nonindigenous introgression among 27 red fox *Vulpes vulpes* samples collected in the northern Greater Yellowstone Ecosystem in Montana and Wyoming between 2003 and 2016.
Found at DOI: https://doi.org/10.3996/092017-JFWM-073.S1 (16 KB XLS).

Table S2. Microsatellite genotypes from red foxes *Vulpes vulpes*, including 27 individuals sampled in the northern Greater Yellowstone Ecosystem (GYE) in Montana and Wyoming between 2003 and 2016 across three elevation groups (high: >2,300 m; middle: 1,600–2,300 m; low: <1,600 m); 24 nonindigenous fur farm red fox reference samples collected in California between 1996 and 2010 (Sacks et al. 2016); and 21 indigenous red fox reference samples collected from Rocky Mountain populations in Idaho ($n = 16$) and Nevada ($n = 5$) between 1880 and 2008 (Sacks et al. 2010). We used these to assess relatedness, isolation by distance, and nuclear genetic diversity and population structure across a 1,750-m elevational gradient in the GYE, as well as the degree of indigenous Rocky Mountain ancestry and fur

farm introgression there. Sample identifications (indicating sex [M, male; F, female] and radio collar frequency [live-capture] or nearest landmark [roadkill or harvest] for GYE samples or state of origin and an identifier number for reference samples) and sampling group are listed for all samples, whereas elevation and sample site coordinates are listed for the GYE samples. Diploid genotypes of three-digit alleles are then listed in columns labeled by microsatellite locus (see Table S1).

[a] Individual whose genotypes we excluded from isolation by distance, genetic diversity, population structure, and ancestry analyses after we identified it as a first-order relative of another individual in the dataset.

Found at DOI: https://doi.org/10.3996/092017-JFWM-073.S2 (30 KB XLS).

Table S3. Mitochondrial DNA (mtDNA) data from 27 red foxes *Vulpes vulpes* sampled in the northern Greater Yellowstone Ecosystem in Montana and Wyoming between 2003 and 2016, used in matrilineal ancestry and genetic diversity analyses. Sample identifications indicate sex (M, male; F, female) and radio collar frequency for live-captured individuals or nearest landmark for harvested or roadkilled individuals. The mtDNA haplotype identification nomenclature is consistent with previously published studies (Sacks et al. 2010). The "abridged composite haplotype sequences" provided are variable sites within the 354-bp cytochrome *b* and 342-bp D-loop composites analyzed, followed by columns containing the entire sequences of the cytochrome *b* and D-loop haplotypes, respectively, of that composite.

[a] Individual whose sequence we excluded from the genetic diversity analysis after we identified it as a first-order relative of another individual in the dataset.

Found at DOI: https://doi.org/10.3996/092017-JFWM-073.S3 (24 KB XLS).

Reference S1. Fuhrmann RT. 1998. Distribution, morphology, and habitat use of the red fox in the Northern Yellowstone Ecosystem. Master's thesis. Bozeman: Montana State University.

Found at DOI: https://doi.org/10.3996/092017-JFWM-073.S4 (7.84 MB PDF).

Acknowledgments

References

Allendorf FW, Leary RF, Spruell P, Wenburg JK. 2001. The problems with hybrids: setting conservation guidelines. Trends in Ecology and Evolution 16:613–622.

Aubry K, Statham MJ, Sacks BN, Perrine JD, Wisely SM. 2009. Phylogeography of the North American red fox: vicariance in Pleistocene forest refugia. Molecular Ecology 18:2668–2686.

Bandelt H-J, Forster P, Röhl A. 1999. Median-joining networks for inferring intraspecific phylogenies. Molecular Biology and Evolution 16:37–48.

Bowcock AM, Ruizlinares A, Tomfohrde J, Minch E, Kidd JR, Cavallisforza LL. 1994. High resolution of human evolutionary trees with polymorphic microsatellites. Nature 368:455–457.

Carbyn LN, Watson D. 2001. Translocation of plains bison to Wood Buffalo National Park: economic and conservation implications. Pages 189–204 in Maehr DS, Noss RF, Larkin JL, editors. Large mammal restoration: ecological and sociological challenges in the 21st century. Washington, D.C.: Island Press.

Champagnon J, Elmberg J, Guillemain M, Gauthier-Clerc M, Lebreton J-D. 2012. Conspecifics can be aliens too: a review of effects of restocking practices in vertebrates. Journal of Nature Conservation 20:231–241.

Clayton, J. 2008. Images of America: Red Lodge. Charleston, South Carolina: Arcadia Publishing.

Cole LJ, Shackelford RM. 1943. White spotting in the fox. American Naturalist 77:289–321.

Copeland JP, Cesar E, Peek JM, Harris CE, Long CD, Hunter DL. 1995. A live trap for wolverine and other forest carnivores. Wildlife Society Bulletin 23:535–538.

Crabtree RL. 1998. On the trail of a gray ghost. National Wildlife 36:48–52.

Crabtree RL, Sheldon JW. 1999. Coyotes and canid coexistence in Yellowstone National Park. Chapter 6 in Clark T, Curlee P, Kareiva P, Minta S, editors. Carnivores in ecosystems; the Yellowstone experience. New Haven, Connecticut: Yale University Press.

Earl DA, vonHoldt BM. 2012. STRUCTURE HARVESTER: a website and program for visualizing STRUCTURE output and implementing the Evanno method. Conservation Genetics Resources 4:359–361.

Evanno G, Reghaut S, Goudet J. 2005. Detecting the number of clusters of individuals using the software STRUCTURE: a simulation study. Molecular Ecology 14:2611–2620.

Excoffier L, Laval G, Schneider S. 2005. Arlequin ver. 3.0: an integrated software package for population genetics data analysis. Evolutionary Bioinformatics Online 1:47–50.

Falush D, Stephens M, Pritchard J. 2003. Inference of population structure using multilocus genotype data:

linked loci and correlated allele frequencies. Genetics 164:1567–1587.

Fuhrmann RT. 1998. Distribution, morphology, and habitat use of the red fox in the Northern Yellowstone Ecosystem. Master's thesis. Bozeman: Montana State University (see *Supplemental Material*, Reference S1).

Gariboldi MC, Tunez JI, Failla M, Hevia M, Panebianco MV, Paso Viola MN, Vitullo AD, Cappozzo HL. 2016. Patterns of population structure at microsatellite and mitochondrial DNA markers in the franciscana dolphin (*Pontoporia blainvillei*). Ecology and Evolution 6:8764–8776.

Goslee SC, Urban DL. 2007. The ecodist package for dissimilarity-based analysis of ecological data. Journal of Statistical Software 22(7):1–19.

Hall ER, Kelson KR. 1959. The mammals of North America. New York: The Ronald Press.

Hedrick PW, Allendorf FW, Baker CS. 2013. Estimation of male gene flow from measures of nuclear and female genetic differentiation. Journal of Heredity 104:713–717.

Hersteinsson P, MacDonald DW. 1982. Interspecific competition and the geographical distribution of red and arctic foxes *Vulpes vulpes* and *Alopex lagopus*. Oikos 64:505–515.

Holmes NG, Dickens HF, Neff MW, Mee JM, Sampson J, Binns MM. 1998. Nine canine microsatellites. Animal Genetics 29:477.

Jombart T. 2008. adegenet: a R package for the multivariate analysis of genetic markers. Bioinformatics 24:1403–1405.

Kalinowski ST. 2005. HP-Rare 1.0: a computer program for performing rarefaction on measures of allelic richness. Molecular Ecology Notes 5:187–189.

Kalinowski ST, Wagner AP, Taper ML. 2006. ML-Relate: a computer program for maximum likelihood estimation of relatedness and relationship. Molecular Ecology Notes 6:576–579.

Kamler JF, Ballard WB. 2002. A review of native and nonnative red foxes in North America. Wildlife Society Bulletin 30:370–379.

Lounsberry ZT, Quinn CB, Statham MJ, Angulo CL, Kalani TJ, Tiller E, Sacks BN. 2016. Investigating genetic introgression from farmed red foxes into the wild population in Newfoundland, Canada. Conservation Genetics 18:383–392.

Merson C, Statham MJ, Janecka JE, Lopez RR, Silvy NJ, Sacks BN. 2017. Distribution of native and nonnative ancestry in red foxes along an elevational gradient in central Colorado. Journal of Mammalogy 98:365–377.

Moore M, Brown SL, Sacks BN. 2010. Thirty-one short red fox (*Vulpes vulpes*) microsatellite markers. Molecular Ecology Resources 10:404–408.

Moulton G. 2005. The Journals of the Lewis and Clark Expedition. Lincoln: University of Nebraska Press.

Oklander LI, Mino CI, Fernandez G, Caputo M, Corach D. 2017. Genetic structure in the southernmost populations of black-and-gold howler monkeys (*Alouatta caraya*) and its conservation implications. PLoS ONE 12:e0185867. DOI: https://doi.org/10.1371/journal.pone.0185867.

Ostrander EA, Mapa FA, Yee M, Rine J. 1995. One hundred and one new simple sequence repeat-based markers for the canine genome. Mammalian Genome 6:192–195.

Ostrander EA, Sprague J, Rine GF. 1993. Identification and characterization of dinucleotide repeat $(CA)_n$ markers for genetic mapping in dog. Genomics 16:207–213.

Perrine JD, Campbell LA, Green GA. 2010. Sierra Nevada red fox (*Vulpes vulpes necator*): a conservation assessment. U.S. Forest Service Report. R5-FR-010. Available: https://nrm.dfg.ca.gov/FileHandler.ashx?DocumentID=23994 (July 2018).

Perrine JD, Pollinger JP, Sacks BN, Barrett RH, Wayne RK. 2007. Genetic evidence for the persistence of the critically endangered Sierra Nevada red fox in California. Conservation Genetics 8:1083–1095.

Pritchard JK, Stephens M, Donnelly P. 2000. Influence of population structure using multilocus genotype data. Genetics 155:945–959.

R Core Team. 2013. R: a language and environment for statistical computing. R Foundation for Statistical Computing, Vienna. Available: http://www.R-project.org (July 2018).

Rousset F. 2008. GENEPOP'007: a complete re-implementation of the GENEPOP software for Windows and Linux. Molecular Ecology Resources 8:103–106.

Sacks BN, Brazeal JL, Lewis JC. 2016. Landscape genetics of the nonnative red fox of California. Ecology and Evolution 6:4775–4791.

Sacks BN, Moore M, Statham MJ, Wittmer HU. 2011. A restricted hybrid zone between native and introduced red fox (*Vulpes vulpes*) populations suggests reproductive barriers and competitive exclusion. Molecular Ecology 20:326–341.

Sacks BN, Statham MJ, Perrine JD, Wisely SM, Aubry K. 2010. North American montane red foxes: expansion, fragmentation, and the origin of the Sacramento Valley red fox. Conservation Genetics 11:1523–1539.

Sikes RS, Gannon WL, and Animal Care and Use Committee of the American Society of Mammalogists. 2011. Guidelines of the American Society of Mammalogists for the use of wild mammals in research. Journal of Mammalogy 92:235–253.

Statham MJ, Murdoch J, Janecka J, Aubry KB, Edward CJ, Soursbury CD, Berry O, Wang Z, Harrison D, Pearch M, Tomsett L, Cupasko J, Sacks BN. 2014. Range-wide multilocus phylogeography of the red fox reveals ancient continental divergence, minimal genomic exchange and distinct demographic histories. Molecular Ecology 23:4813–4830.

Statham MJ, Sacks BN, Aubry KB, Perrine JD, Wisely SM. 2012. The origin of recently established red fox populations in the contiguous United States: translo-

cations or natural range expansions? Journal of Mammalogy 93:52–65.

Swanson BJ, Fuhrmann RT, Crabtree RL. 2005. Elevational isolation of red fox populations in the Greater Yellowstone Ecosystem. Conservation Genetics 6:123–131.

Toews DPL, Brelsford A. 2012. The biogeography of mitochondrial and nuclear discordance in animals. Molecular Ecology 21:3907–3930.

Toonen RJ, Hughes S. 2001. Increased throughput for fragment analysis on an ABI PrizmH 377 automated sequencer using a membrane comb and STRand software. BioTechniques 31:1320–1324.

[ESA] U.S. Endangered Species Act of 1973, as amended, Pub. L. No. 93-205, 87 Stat. 884 (Dec. 28, 1973). Available: http://www.fws.gov/endangered/esa-library/pdf/ESAall.pdf (July 2018).

[USFWS] U.S. Fish and Wildlife Service. 2015. 12-Month finding on a petition to list Sierra Nevada red fox as an endangered or threatened species. Federal Register 80(195):60989–61028.

Van Etten KW, Wilson KR, Crabtree RL. 2007. Habitat use of red foxes in Yellowstone National Park based on snow tracking and telemetry. Journal of Mammalogy 88:1498–1507.

Volkmann LA, Statham MJ, Mooers AØ, Sacks BN. 2015. Genetic distinctiveness of red foxes in the Intermountain West as revealed through expanded mitochondrial sequencing. Journal of Mammalogy 96:297–307.

Waples RS, Anderson EC. 2017. Purging putative siblings from population genetic data sets: a cautionary view. Molecular Ecology 26:1211–1224.

Witte SS, Gallagher MV. 2012. The North American journals of Prince Maximilian of Wied, Vol. III. Norman: University of Oklahoma Press.

Wright, S. 1943. Isolation by distance. Genetics 28:114–138.